X-932-74-90

PREPRINT

NASA TM X- 70637

STRATEGIES FOR ESTIMATING THE MARINE GEOID FROM ALTIMETER DATA

P. ARGENTIERO
W. D. KAHN
R. GARZA-ROBLES

APRIL 1974

GSFC

GODDARD SPACE FLIGHT CENTER
GREENBELT, MARYLAND

Presented at the National Spring Meeting of the American Geophysical Union, April 8-12, 1974, Washington, D. C.

X-932-74-90

STRATEGIES FOR ESTIMATING THE MARINE GEOID FROM ALTIMETER DATA

P. Argentiero
W. D. Kahn
R. Garza-Robles

April 1974

Presented at the National Spring Meeting of the American Geophysical Union
April 8-12, 1974, Washington, D. C.

GODDARD SPACE FLIGHT CENTER
Greenbelt, Maryland

STRATEGIES FOR ESTIMATING THE MARINE GEOID FROM ALTIMETER DATA

P. Argentiero
W. D. Kahn
R. Garza-Robles

ABSTRACT

In processing altimeter data from a spacecraft borne altimeter to estimate the fine structure of the marine geoid, a problem is encountered. In order to describe the geoid fine structure, a large number of parameters must be employed and it is not possible to simultaneously estimate all of them. In practice, one is forced to hold a large number of parameters at a priori values and adjust others. Unless the parameterization exhibits good orthogonality in the data, serious aliasing results. From simulation studies it has been found that amongst several competing parameterizations, the mean free air gravity anomaly model (i.e., Stokes' formula) exhibited promising geoid recovery characterisitics.

Using covariance analysis techniques, this paper provides quantitative measures of the orthogonality properties associated with the above mentioned parameterization. For instance, it has been determined that a 5° x 5° area mean free air gravity anomaly can be estimated with an uncertainty of 1 mgal (40 cm undulation) provided that all free air gravity anomalies within a spherical radius of 10 arc degrees are simultaneously estimated.

CONTENTS

ILLUSTRATIONS

STRATEGIES FOR ESTIMATING FROM ALTIMETER DATA THE MARINE GEOID

INTRODUCTION

The primary function of the spacecraft borne altimeter is to determine the fine structure of the mean sea surface topography. The instrument is well suited for the task. Consider, for instance, the altimeter which will be on board the GEOS-C spacecraft which is scheduled for launch in late 1974. In its global mode the instrument will be capable of producing a measurement every four kilometers along the subearth path of the satellite. This implies that even assuming considerable data compression it will be mathematically possible to extract from such data topographic detail of one degree or less.

But there are practical difficulties to be overcome if the full potential of altimetry as a data type can be realized. To see what these difficulties are it is necessary to closely analyze what happens when standard estimation techniques are employed to obtain sea surface topography from altimetry data. Essentially the problem is to reconstruct an analytic surface from direct but noisy observations of the surface taken at specified points. The obvious approach is to parameterize the surface in terms of coefficients which define a suitably dense set of functions in the space of two dimensional analytic functions and to recover the coefficients from the data by means of a standard minimum variance filter. Often the physical setting of the problem suggests the proper parameterization. If not, then an arbitrary family of analytic functions such as the set of two dimensional polynomials can be used. For this problem a natural parameterization is suggested by the fact that after suitable corrections the mean sea surface can be considered as cohering closely to an equipotential surface known as the marine geoid. (1) Thus one candidate for a natural parameterization is the set of standard spherical harmonic coefficients of the Earth's geopotential field.

It is certain that any parameterization capable of describing the fine structure of the surface in question must employ an enormous number of coefficients. For instance, if we are interested in three degree features of the marine geoid and if the standard spherical harmonic expansion of the geopotential field is used as a parameterization, a full set of coefficients up to degree and order 60 would be required. This implies the estimation of over 3700 parameters! Unless very special circumstances apply it is not possible to simultaneously estimate such large parameter sets. In practice, in order to use parameter estimation techniques in recovering the marine geoid fine structure from altimeter data it will be necessary to adjust small subsets of the parameters while in effect "freezing" the rest at a priori values. But unless the parameterization exhibits a certain property with regard to altimetry data which we term "orthogonality in

the data set", the net effect will be that the uncertainties in the adjusted terms will badly corrupt the estimates of the adjusted terms. This effect is frequently called aliasing. The orthogonality property just mentioned will be rigorously defined in a later section but in essence it is a property of a parameterization which permits a decomposition of the estimation problem into estimation problems of much smaller dimensionality and without fear of serious aliasing.

To take full advantage of the attractive properties of altimetry it will be necessary to develop a parameterization of the marine geoid which exhibits good orthogonality properties in altimeter data. The orthogonality properties of the set of spherical harmonic coefficients of the geopotential field is very poor and it is not a good candidate for the proper parameterization. Other candidates for the parameterization of the marine geoid are surface density layers (2) and sample functions (3). The parameterization whose properties will be investigated in this paper is the one provided by mean free air gravity anomalies and Stokes' formula (4), (5). If this parameterization is to be used to determine the marine geoid from altimeter data it will be important to discover to what extent mean free air gravity anomalies are orthogonal in the data. Specifically, we would like to know how far two mean free air gravity anomalies must be separated before one can be sure that a neglecting of one anomaly does not badly alias the estimate of the other. Without knowledge of this distance it is impossible to make intelligent use of the parameterization.

The results of the SKYLAB altimeter experiment have demonstrated the ability of altimetry to reveal marine geoid fine structure. But it will be during the GEOS-C mission that for the first time scientists will have an opportunity to examine the output of a spacecraft borne altimeter functioning in a global mode over the world's oceans. In the succeeding section the performance of the SKYLAB altimeter and the goals of the GEOS-C experiment will be discussed. Next, the mathematical details of the measurement modeling and preprocessing of altimeter data will be described and the Stokes' formula mean free air gravity anomaly parameterization of the marine geoid will be documented. Following that will be a detailed discussion of the dual concepts of orthogonality and aliasing and their relationships to the problem of estimating a marine geoid from altimeter data. Finally, the results of a systematic application of covariance analysis will be used to develop optimal estimation strategies for determining the marine geoid from altimetry data.

THE SKYLAB AND GEOS-C ALTIMETER EXPERIMENTS

The GEOS-C spacecraft will be inserted into orbit during the latter part of calendar year 1974. This spacecraft will have as its prime experiment, a radar altimeter. The objectives of the GEOS-C altimeter experiment are: (a) to determine the feasibility and utility of a spaceborne altimeter to map the topography of the ocean surface with an absolute height accuracy of ±5 meters, and with a relative height accuracy of 1 to 2 meters, (b) to determine the feasibility of measuring the deflections of the vertical at sea, (c) determine the feasibility of measuring wave height, and (d) contribute to technology leading to a future operational satellite altimeter system with a 10 cm measurement capability.

The altimeter data, when calibrated and corrected e.g., for sea state, ocean tides, and other effects, constitute measures of the distance between the GEOS-C spacecraft and the ocean surface. Knowledge of the satellite altitude relative to a reference ellipsoid and knowledge of the oceanographic departures of the sea surface topography from the geoid will then permit the determination of the geoid. The chief problem is expected to be the determination of orbital altitude for GEOS-C. The primary tracking systems for doing this are the satellite to satellite tracking system and precision lasers. Data from these systems and others tracking GEOS-C, including C-band radars, USB range and range rate stations, and TRANET Doppler stations, will be used to find satellite height.

Satellite contributions to the determination of the current ocean geoid have spatial resolutions corresponding to half wavelengths of approximately 18° (i.e., 2000 km). Surface gravity achieves representations with finer resolution, in the 1° to 5° range (i.e., 110 km to 550 km), however it covers only about 50% of the ocean surface. The GEOS-C altimeter system will thus fill in the gaps and provide valuable independent knowledge where data now exist.

The ability of a radar altimeter to detect features of the ocean surface has recently been demonstrated by the SKYLAB altimeter. In Figure 1 an altimeter pass over the Puerto Rican Trench has been analyzed. The pass was over the southwest corner of Puerto Rico and was 72.8 seconds in duration. From a plot of the height residuals (formed by comparing the altimeter measurements with the calculated height of SKYLAB's orbit) it can be seen that a 17 meter drop in height residuals occurs when SKYLAB passed over the deepest part of the ocean (i.e., corresponding to a 4000 meter depth of the ocean bottom) and the peaking of the height residuals occurred when SKYLAB traversed the Puerto Rican land mass. The SKYLAB data described here exemplifies the high level of resolution of surface features by a radar altimeter.

It is to be pointed out however, that data from the GEOS-C experiment will be significantly free of the effects of spacecraft dynamic motions

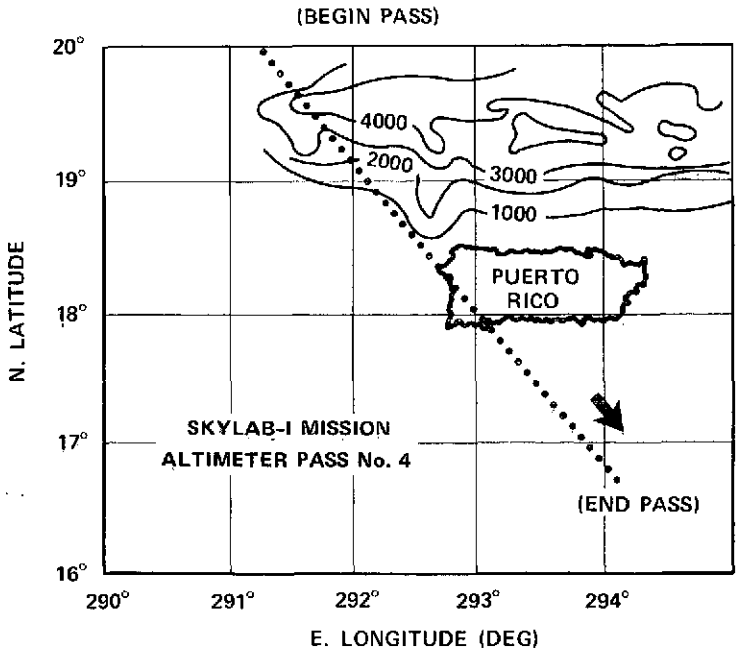

(A) GROUND TRACK OF ALTIMETER PASS

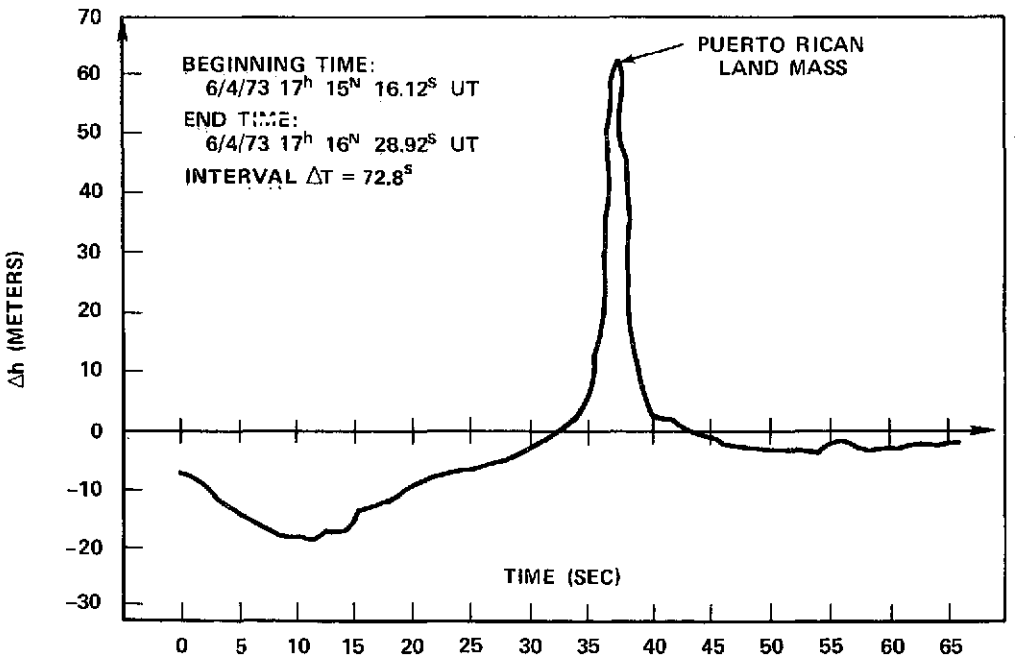

(B) SKYLAB I ALTIMETER RESIDUALS VS TIME
DATA SOURCE: NASA WALLOPS STATION

Figure 1.

which is not the case for SKYLAB altimeter data, since in the latter there were attitude control jet thrusting, crew motion, etc. In addition, because GEOS-C will have a nominal 1 year operating lifetime the altimetry data obtained will be far in excess of that obtained from SKYLAB. Thus for reasons cited above, the GEOS-C altimeter experiment data is most suitable for improving the marine geoid.

To successfully utilize GEOS-C altimetry data for improving the accuracy of the marine geoid, dictated the development of unique computer programs capable of processing these data. The descriptions of the mathematical models associated with these programs and the computation strategies for processing altimeter data are provided in succeeding sections.

DESCRIPTION OF THE ALTIMETER MEASUREMENT

The geometry associated with the altimeter measurement is described in Figure 2. As can be seen, the altimeter measurement is nominally the shortest distance between the satellite and the sea surface, that is, the measurement is along the normal to the sea surface that passes through the satellite. The mathematical model for the altimeter measurement is given by the following relationship:

$$h_a = h - N' - \delta h_s - \Delta h' \tag{1}$$

where

$h \equiv |\vec{\rho} - \vec{r}_{se}|$

$\vec{\rho} \equiv$ position vector of S/C

$\vec{r}_{se} \equiv$ geocentric radius vector

$N' \equiv$ geoid height above reference ellipsoid

$\delta h_s \equiv$ deviation of sea surface from geoid

$\Delta h \equiv$ systematic errors in altimeter measurement (e.g., refraction, timing, etc.)

A more detailed description of the mathematical modelling of the altimeter measurement is given in Reference 6 (pp. 4-3 to 4-13).

The error sources that effect the altimeter measurement fall into three categories: those that are due to orbit uncertainty, those that cause the measured geoid to deviate from the true geoid, and those that effect the measurement accuracy itself. Equation 2 below describes the functional dependence of the error sources on the altimeter measurement:

$$h_a = h(\vec{E}_0 t) - N'(\vec{G}_0) - \delta h_s(\vec{\tau}_0, \vec{s}_0, \phi, \lambda, t) - \Delta h'(\vec{m}_0, \phi, \lambda, t) \tag{2}$$

where

h: S/C altitude above reference ellipsoid

E: orbit parameters and orbit dependent terms (radiation pressure, drag, etc.)

t: time of altimeter measurement

$\vec{G}_0$: vector of geopotential coefficients

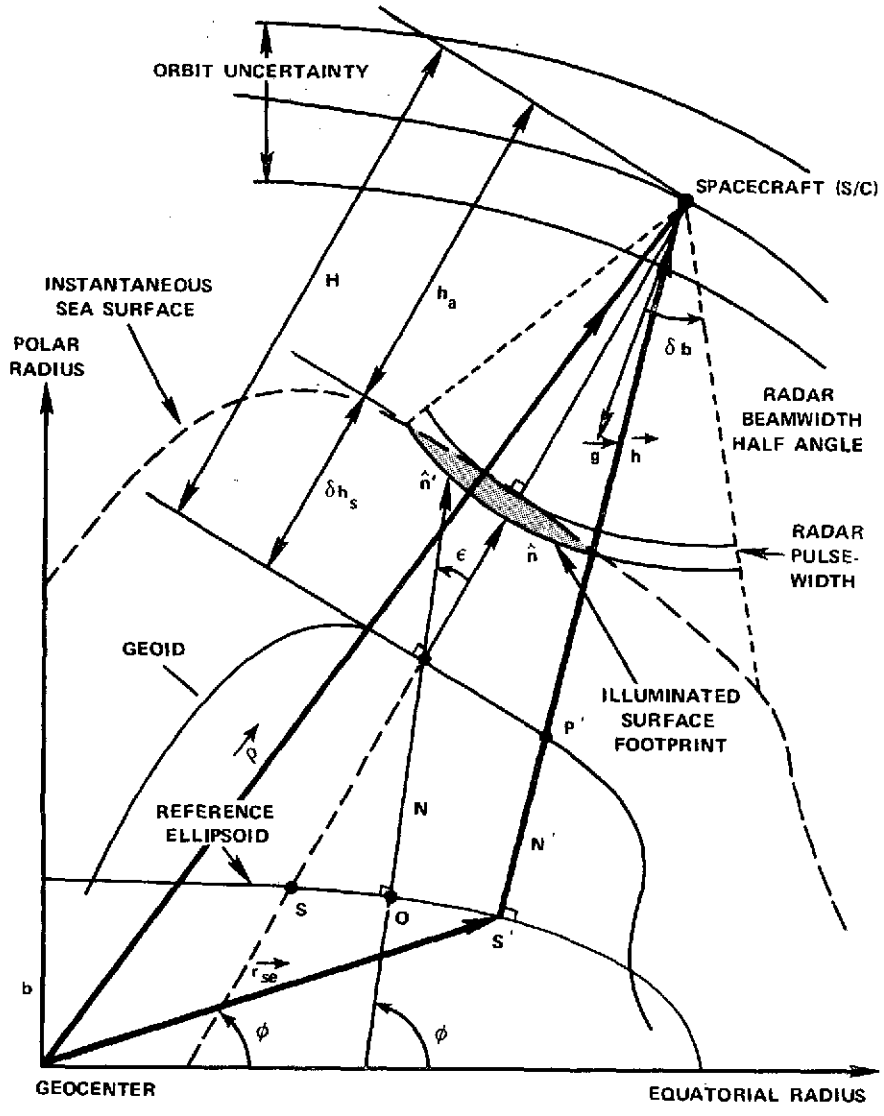

$\vec{\rho} = \vec{r}_{se} + \vec{h}$

$\vec{h} = \vec{\rho} - \vec{r}_{se}$

$h = |\vec{h}| = N' + h_a + \delta h_s + \Delta h'$

$h_a = h - N' - \delta h_s - \Delta h'$

WHERE:

- $\vec{\rho}$: POSITION VECTOR OF S/C
- $\hat{n}$: VECTOR FROM S' ON REFERENCE ELLIPSOID TO S/C
- $\vec{r}_{se}$: GEOCENTRIC RADIUS VECTOR TO POINT S' ON REFERENCE ELLIPSOID.
- h : MAGNITUDE OF $\vec{h}$
- h_a : S/C ALTITUDE ABOVE SEA SURFACE
- N' : GEOID HEIGHT ABOVE REFERENCE ELLIPSOID
- δh_s : DEVIATION OF SEA SURFACE FROM GEOID
- Δh : SYSTEMATIC ERRORS IN ALTIMETER MEASUREMENT, e.g., REFRACTION, ANTENNA OFFSET, TIMING, ETC.

Figure 2. Altimeter Measurement Geometry

N': geoid undulation function

$\vec{\tau}_0$: vector of tidal error model coefficients

$\vec{s}_0$: vector of local sea surface biases (i.e., currents, storm surges, wind waves...)

$\vec{m}_0$: vector of altimeter measurement error coefficients

or in general

$$h_a = h_a(\vec{E}_0, \vec{G}_0, \vec{\tau}_0, s_0, \vec{m}_0, \phi, \lambda, t) \tag{3}$$

The altimeter measurement will be corrected for known error sources, smoothed, sorted, etc. by the data preprocessor. Then, each measurement will be compared with altitude calculated from the satellite's orbit (h'_a) to form the measurements residual Δh_a:

$$\Delta h_a = h_a - h'_a \tag{4}$$

Mathematically, this residual is equivalent to the difference function,

$$\begin{aligned} \Delta h_a = & \frac{\partial h_a}{\partial E_i} \Delta E^i + \frac{\partial h_a}{\partial G_j} \Delta G^j + \frac{\partial h_a}{\partial \tau_k} \Delta \tau^k \\ & + \frac{\partial h_a}{\partial s_\ell} \Delta s^\ell + \frac{\partial h_a}{\partial m_r} \Delta m^r + \epsilon \end{aligned} \tag{5}$$

or

$$\Delta h_a = \Delta h_a(E) + \Delta h_a(G) + \Delta h_a(\tau) + \Delta h_a(s) + \Delta h_a(m) \tag{5a}$$

The models for the altimeter measurement errors are now to be specified.

1. Error Due to Orbital Parameters $\Delta h_a(E)$

Precision laser tracking data, Satellite to Satellite Tracking (SST), USB, C-Band and Doppler data preceding and during altimeter measurement data acquisition will be used to correct the error on altimeter measurements due to orbital parameters using an existing orbit determination program. Orbit height accuracy required for altimetry data reduction must be better than 1 meter. Recent studies indicate that this is feasible (Ref. 7).

2. Error Due to Tides and Sea Surface $\Delta h_a(\tau)$ and $\Delta h_a(s)$

Corrections for deviations from the geoid due to ocean tides are based on the model of Hendershott (Ref. 8). In this model the dominant lunar semi-diurnal tide (M_2) with lunar declination terms neglected is represented. This tidal model is representative of the current state of the art. The maximum error contribution due tides is approximately 1 meter. The contributions due to local sea surface biases is on the order of 50 cm, below the resolution threshold of the GEOS-C altimeter. Therefore sea surface bias corrections are neglected.

3. Errors Due to Altimeter Hardware $\Delta h_a(m)$

Altimeter measurement errors which directly affect the accuracy for determining the geoid radius are:

$$\Delta h_a(m) = \Delta h_0 + \Delta h_\ell + \Delta h_L + \Delta h_D + \Delta h_T + \Delta h_R \tag{6}$$

where

Δh_0: altimeter antenna offset

Δh_ℓ: antenna offset due to S/C libration

Δh_L: dynamic lag

Δh_D: altimeter drift

Δh_T: timing bias

Δh_R: tropospheric refraction

Models for the above error sources are now described.

A. Altimeter Antenna Offset

$$\Delta h_0 = h_a \tan \tfrac{1}{2}(\alpha_0 - \delta_b) \tan(\alpha_0 - \delta_b) + \left[\frac{(c\tau)^3}{4\delta_b h_a}\right]^{1/2} \left[\left(\frac{\alpha_0}{2\delta_b}\right)^2 - .225\right] \tag{6a}$$

for

$$\delta_b \leq \alpha_0 < 2^\circ$$

or

$$\Delta h_0 = \left[\frac{(c\tau)^3}{4\delta_b^2 h_a}\right]^{1/2} \left[\left(\frac{\alpha_0}{2\delta_b}\right)^2 - .225\right] \tag{6b}$$

for

$$0 < \alpha_0 < \delta_b$$

where

h_a: spacecraft altitude

δ_b: antenna half beamwidth angle

α_0: angle off boresight

τ: transmitted pulse length

c: velocity of light (299.7925×10^3 km/sec)

B. Antenna Offset Due to S/C Libration

$$\Delta h_\ell = h_a \tan \tfrac{1}{2}(\alpha_\ell - \delta_b) \tan(\alpha_\ell - \delta_b) + \left[\frac{(c\tau)^3}{4\delta_b h_a}\right]^{1/2} \left[\left(\frac{\alpha_0}{2\delta_b}\right)^2 - .225\right] \tag{6c}$$

for

$$\delta_b \leqslant \alpha_\ell < 2^\circ$$

or

$$\Delta h_\ell = \left[\frac{(c\tau)^3}{4\delta_b^2 h_a}\right]^{1/2} \left[\left(\frac{\alpha_\ell}{2\delta_b}\right)^2 - .225\right] \tag{6d}$$

for

$$0 < \alpha_\ell < \delta_b$$

where

$$\alpha_\ell = A_\ell \sin\left(\frac{2\pi}{T} t + \phi_\ell\right)$$

α_ℓ: S/C libration angle

A_ℓ: peak libration angle

ϕ_ℓ: libration phase angle

T: orbital period.

C. Dynamic Lag

A measurement bias error induced by the change in S/C position at the time of the outgoing and return pulses.

$$\Delta h_L = \frac{\dot{h}_{i+1} - \dot{h}_i}{(t_{i+1} - t_i)} \mathcal{L} \tag{6e}$$

where

$\dot{h}_i$: altitude rate at time t_i (sec)

$\mathcal{L}$: lag coefficient (sec^2)

D. Altimeter Drift

A measurement bias error due to component aging.

$$\Delta h_D = D(t - t_0) \tag{6f}$$

where

t_0: initial time of altimeter measurement

t: current time of altimeter measurement

D: drift coefficient (sec)

E. Timing Bias

Bias error introduced by S/C clock error.

$$\Delta h_T = \dot{h}\tau \tag{6g}$$

$\dot{h}$: height rate at time of altimeter measurement

τ: clock error coefficient

F. Tropospheric Refraction Error

Bias error introduced into altimeter measurement due to tropospheric refraction. The Model used is that developed by J. Saastamoinen (Ref. 9).

4. Error Due to Geopotential $\Delta h_a(G)$

In the preprocessing of altimeter data the altimeter measurement will have been corrected for the orbit uncertainties ocean tides, local sea surface biases and measurement bias errors using the error models described above. Thus Equation 4 above is restated as follows:

$$\Delta h_a(G) = h_a - [h'_a + \Delta h_a(E) + \Delta h_a(\tau) + \Delta h_a(s) + \Delta h_a(m)] \tag{7}$$

And the relationship between altimeter measurement residuals to geoidal parameters can then be stated as follows:

$$\Delta h_a(G) \approx \frac{\partial h_a}{\partial G_j} \Delta G_j. \tag{8}$$

As stated above, the altimeter measurement residual as described in (7) solely reflects primarily (neglecting second order effects) the departure of the geoid from the reference ellipsoid. Or more precisely the distance along the UNIT normal to the reference ellipsoid between the reference ellipsoid and the geoid which is called geoidal height or geoidal undulation N′ (see Figure 2).

The mathematical relationship which relates the geoidal undulation to the disturbing potential T is given by Bruns' formula derived in Reference 4. That is

$$N = \frac{T}{\gamma} \tag{9}$$

where

$T \equiv$ disturbing potential

$\gamma \equiv$ magnitude of gravity vector normal to reference ellipsoid

The disturbing potential of the global geoid at point (ϕ, λ, r) is expressed in terms of spherical harmonics as follows:

$$T = \frac{GM}{r} \sum_{n=2}^{L} \left(\frac{a}{r}\right)^n \sum_{m=0}^{n} P_{nm}(\sin \phi) \left[C_{nm} \cos m\lambda + S_{nm} \sin m\lambda\right] \qquad (10)$$

where

GM:	gravitational constant of the earth
C_{nm}, S_{nm}:	spherical harmonic expansion coefficients
$P_{nm}(\sin \phi)$:	associated legendre functions
(ϕ,λ):	latitude and longitude on geoid at which disturbing potential is evaluated
r:	geocentric radius from earth center of mass to evaluation point of disturbing potential on geoid
a:	semi-major axis of reference ellipsoid
L:	is the limit of summation, and it is specified by the degree of harmonic expansion of the global geoid
n:	summation index for degree terms of the spherical harmonic expansion of T
m:	summation index for the order of terms in spherical harmonic expansion of T

Thus the geoidal undulation at any point P (ϕ, λ, r) on the earth can be computed from geopotential coefficients derived from satellites by analysis of perturbations on the orbits induced by the earth's gravity field. The undulations are computed from the combination of Equations 9 and 10.

Another form of expressing the disturbing potential is in terms of Stokes' formula (Ref. 4 pp. 92-98). This formula makes it possible to express the disturbing potential of the global geoid from gravity data. That is

$$T = \frac{R}{4\pi} \int_{\sigma} \int \Delta g \, S(\psi) \, d\sigma \qquad (11)$$

where

$$R = a(1 - f)^{1/3}$$

a: radius of reference ellipsoid

f: flattening of reference ellipsoid

$S(\psi) \equiv$ Stokes' function

σ: element of area

Δg: surface gravity anomalies

$$S(\psi) \equiv \csc\left(\frac{\psi}{2}\right) - 6\sin\frac{\psi}{2} + 1 - 6\cos\psi - 3\cos\psi\,\ln\left(\sin\frac{\psi}{2} + \sin^2\frac{\psi}{2}\right) \qquad (11a)$$

from Bruns' formula (Eq. 9).

The geoidal undulation at any point P on the global geoid can be computed from Stokes' formula (Eq. 11). That is

$$N = \frac{T}{\gamma} = \frac{R}{4\pi\gamma}\int_{\sigma}\int \Delta g\, S(\psi)\, d\sigma \qquad (11b)$$

In terms of geographical coordinates Stokes' function can be expressed as follows:

$$N(\phi,\lambda) = \frac{R}{4\pi\gamma}\int_{\lambda'=0}^{2\pi}\int_{\phi'=-\pi/2}^{\pi/2} \Delta g(\phi',\lambda')\, S(\psi)\cos\phi' d\phi' d\lambda' \qquad (11c)$$

where

$$d\sigma = \cos\phi' d\phi' d\lambda'$$

$(\phi,\lambda) \equiv$ latitude and longitude of the computation point

$(\phi'\lambda') \equiv$ coordinates of the variable surface element σ

ψ: spherical distance between the computation point and variable surface element

$$\psi = \cos^{-1}[\sin\phi\sin\phi' + \cos\phi\cos\phi'\cos(\lambda - \lambda')]$$

$\Delta g(\phi'\lambda')$: free air gravity anomaly at the variable point $(\phi'\lambda')$

$\Delta g(\phi'\lambda')$: free air gravity anomaly at the variable point $(\phi'\lambda')$

γ: mean value of gravity over earth

In order to combine surface gravity data and geopotential information derived from gravity field perturbations acting on orbits of spacecraft, the earth is divided into two areas (see Ref. 10), a global area (A_1) and a local area (A_2), surrounding the point P. Each gravity anomaly in each area is also partitioned into two parts represented by Δg_s and Δg_2 respectively where

$$\Delta g_s = \gamma \left[\sum_{n=2}^{L} \sum_{m=0}^{n} (n-1) \left(\frac{a}{r}\right)^n P_{nm}(\sin\phi) \{C_{nm} \cos n\lambda + S_{nm} \sin m\lambda\} \right] \quad (11d)$$

$$\Delta g_s = \gamma \left[\sum_{n=2}^{L} \sum_{m=0}^{n} (n-1) \left(\frac{a}{r}\right)^n P_{nm}(\sin\phi) \{C_{nm} \cos n\lambda + S_{nm} \sin m\lambda\} \right] \quad (11d)$$

The Δg_2 value is defined as the remainder of the gravity anomaly. By partitioning the earth into two areas and the geoidal undulations into two components. Equation 11c can thus be rewritten as follows:

$$N(\phi,\lambda) = N_1 + N_2 \quad (11e)$$

$$N(\phi,\lambda) = N_1 + N_2 \quad (11e)$$

where

$$N_1 = \frac{R}{4\pi\gamma} \int_0^{2\pi} \int_{-\pi/2}^{\pi/2} \Delta g_s(\phi',\lambda') S(\psi) \cos\phi' d\phi' d\lambda'$$

$$N_1 = \frac{R}{4\pi\gamma} \int_0^{2\pi} \int_{-\pi/2}^{\pi/2} \Delta g_s(\phi',\lambda') S(\psi) \cos\phi' d\phi' d\lambda'$$

or

$$= \frac{T}{\gamma}$$

$$= \frac{T}{\gamma}$$

and

$$N_2 = \frac{R}{4\pi\gamma} \int_{A_2} \int \Delta g_2(\phi',\lambda') S(\psi) \cos\phi' d\phi' d\lambda'$$

$$N_2 = \frac{R}{4\pi\gamma} \int_{A_2} \int \Delta g_2(\phi',\lambda') S(\psi) \cos\phi' d\phi' d\lambda'$$

$$N_2 = \Delta N_1 = \delta\tilde{N} = \frac{\Delta T}{\gamma}$$

$$N_2 = \Delta N_1 = \delta\tilde{N} = \frac{\Delta T}{\gamma}$$

$$\Delta g_2 = \delta(\Delta g_s)$$

$$\Delta g_2 = \delta(\Delta g_s)$$

Thus

$$N(\phi,\lambda) = \frac{T + \Delta T}{\gamma} \tag{11f}$$

$$N_2 = \Delta N_1 = \frac{R\,\Delta\phi'\Delta\lambda'}{4\pi\gamma} \sum_{j=1}^{\bar{L}} \delta\{\Delta g_s(\phi_j'\lambda_j')\}\, S(\psi_j) \cos\phi_j'$$

where ΔN_1 is the correction to the geoidal undulations of the global geoid as a function of the corrections of mean free air gravity anomalies.

Equation 11f is the form of the parameterization adapted for relating the altimeter measurement residuals to geoidal parameters. That is, Equation 8 can now be written as follows:

$$\delta\tilde{N} = \Delta h_a = \Delta N_1$$

$$\delta\tilde{g} = \Delta G_j = \delta\{\Delta g_s(\phi_j'\lambda_j')\} \tag{12}$$

$$A = \frac{\partial h_a}{\partial G_j} = \frac{R\,\Delta\phi'\Delta\lambda'}{4\pi\gamma} S(\psi_j) \cos\phi_j'$$

or in the matrix form

$$\delta\tilde{N}_{(k \times 1)} = A_{(k \times j)}\, \delta\tilde{g}_{(j \times 1)} \tag{12a}$$

ORTHOGONALITY AND ALIASING

Assuming that altimeter observations can be directly translated into deviations of the marine geoid from a reference geoid, it is straightforward to estimate gravity anomalies from altimetry data. Let $\delta\tilde{N}$ be a vector of geoid undulations collected from a certain region over the ocean. Next let $\delta\tilde{g}$ be a vector of mean free air gravity anomalies defined over a region of the ocean which contains the data region. Then repeating Equation 12 we have

$$\delta\tilde{N} = A\,\delta\tilde{g} \tag{13}$$

where A is a matrix the number of whose rows is equal to the number of data points and the number of whose columns is equal to the number of gravity anomalies. As demonstrated in Eq. 12 the individual elements of A, say A (I, J), can be computed through Stokes' formula and the latitude and longitude of the i^{th} data point together with the longitude and latitude of the midpoint of the grid over which the J^{th} gravity anomaly is defined. Equation 13 provides a linear equation of condition and in a standard minimum variance fashion $\delta\tilde{g}$ could be estimated from observations of $\delta\tilde{N}$. But in order for Equation 13 to be correct (correct, that is, assuming that the approximations inherent in the discrete form of Stokes' formula are valid) the gravity anomalies in the array $\delta\tilde{g}$ must cover the globe. Considerably smaller regions would no doubt be adequate but just how small these regions can be before a serious bias is introduced into the estimation process is a matter to be determined from computations. In any case, computational consideration constrain us to chose a region such that the number of elements in the $\delta\tilde{g}$ array does not exceed two or three hundred. Gravity anomalies outside of this region are in effect assumed to be zero. To see precisely what happens when this assumption is made, postulate that the $\delta\tilde{g}$ array of Equation 13 is defined over an area sufficiently large that Equation 13 is substantially correct. Then write

$$\delta\tilde{g} = \begin{bmatrix} \delta\tilde{g}_1 \\ \hline \delta\tilde{g}_2 \end{bmatrix} \tag{14}$$

where

$\delta\tilde{g}_1$ = gravity anomalies to be adjusted in a standard minimum variance filter

and

$\delta\tilde{g}_2$ = gravity anomalies assumed to be zero and thus left unadjusted by the minimum variance filter.

Then Equation 13 can be written

$$\delta\tilde{N} = A_1\,\delta\tilde{g}_1 + A_2\,\delta\tilde{g}_2 \tag{15}$$

where A_1 and A_2 are respectively the variational matricies of $\delta\tilde{N}$ with respect to $\delta\tilde{g}_1$ and with respect to $\delta\tilde{g}_2$.

After proper corrections altimeter data is treated as direct observations δN of $\delta\tilde{N}$ with statistics

$$\delta N = \delta\tilde{N} + \nu,\ E(\nu) = \bar{0},\ E(\nu\nu^T) = Q \tag{16}$$

Estimates of mean free air gravity anomalies obtained from satellite tracking and gravimetry measurements are available.[10] Unless this information were correctly factored into the gravity anomaly estimates obtained from altimeter data, the resultant estimates would not be optimal. Consequently we assume the existence of an a priori estimate $\delta g_1'$ of $\delta\tilde{g}_1$ with properties

$$\delta g_1' = \delta\tilde{g}_1 + \alpha_1,\ E(\alpha_1) = \bar{0},\ E(\alpha, \alpha_1^T) = P_1 \tag{17}$$

The gravity anomalies $\delta\tilde{g}_2$ for computational reasons are assumed to be zero but the actual values of gravity anomalies in the region on the sphere which is ignored have a certain distribution about zero. We assume

$$E(\delta\tilde{g}_2) = \bar{0},\ E(\delta\tilde{g}_2\,\delta\tilde{g}_2^T) = P_2 \tag{18}$$

When the values of $\delta\tilde{g}_2$ are assumed to be zero the minimum variance estimate of $\delta\tilde{g}_1$ becomes

$$\delta\hat{g}_1 = (A_1^T Q^{-1} A_1 + P_1^{-1})^{-1}\,[A_1^T Q^{-1}\,\delta N + P_1^{-1}\,\delta g_1'] \tag{19}$$

See Reference 11 for details. Define the covariance matrix of the estimator given by equation 19 as

$$P = E\,[(\delta\hat{g}_1 - \delta\tilde{g}_1)\,(\delta\hat{g}_1 - \delta\tilde{g}_1)^T] \tag{20}$$

From Equations 15, 16, 17 and 19 we obtain

$$\delta\hat{g}_1 - \delta\tilde{g}_1 = (A_1^T Q^{-1} A_1 + P_1^{-1})^{-1}\,(-A_1^T Q^{-1} A_2\,\delta\tilde{g}_2 + A_1^T Q^{-1}\,\nu + P_1^{-1}\,\alpha_1) \tag{21}$$

Equation 21 yields

$$\begin{aligned} P = {} & (A_1^T Q^{-1} A_1 + P_1^{-1})^{-1} + (A_1^T Q^{-1} A_1 P_1^{-1})^{-1}\,A_1^T Q^{-1} A_2 P_2 A_2^T Q^{-1} A_1 \\ & (A_1^T Q^{-1} A_1 + P_1^{-1})^{-1} \end{aligned} \tag{22}$$

Assume that the data is uncorrelated and that each data point has the same variance. Then

$$Q = I\sigma_0^2 \tag{23}$$

Where I is the identity matrix and σ_0^2 is the common variance of the data. Also assume that the values of the unadjusted gravity anomalies are independently distributed. Then the covariance matrix P_2 of $\delta\tilde{g}_2$ can be written as

$$P_2 = \begin{bmatrix} \sigma_1^2 & & & \\ & \sigma_2^2 & & 0 \\ & & \ddots & \\ 0 & & & \sigma_{n_2}^2 \end{bmatrix} \tag{24}$$

Where n_2 is the number of unadjusted gravity anomalies and σ_i^2 is the second moment about zero of the i^{th} unadjusted gravity anomaly.

Also define a matrix K as

$$K \equiv (A_1^T Q^{-1} A_1 + P_1^{-1})^{-1} A_1^T Q^{-1} A_2 \tag{25}$$

If n_1 is the number of adjusted parameters, then K is of dimension n_1 by n_2. With these assumptions Equation 22 yields the following expression for the variance of the i^{th} adjusted gravity anomaly

$$P(I,I) = \sum_{j=0}^{n_2} (\beta_{i,j}\,\sigma_j)^2 \tag{26}$$

Where $\beta_{i,0}^2$ is the i^{th} diagonal element of the matrix $(A_1^T A_1)^{-1}$ (we assume here that diagonal elements of the matrix P_1^{-1} are relatively small) and

$$\beta_{i,j} = K(I,J),\ J \geqslant 1 \tag{27}$$

Define the error sensitivity matrix as

$$s = \{\beta_{i,J}\},\ i = 1,2,\ldots n_1,\ J = 0,1,2,\ldots n_2 \tag{28}$$

and finally define the Alias Matrix as

$$L \equiv s\tilde{\sigma} \tag{29}$$

where

$$\bar{\sigma} \equiv \begin{bmatrix} \sigma_0 & & & & \\ & \sigma_1 & & 0 & \\ & & \sigma_2 & & \\ & & & \ddots & \\ & 0 & & & \\ & & & & \sigma_{n_2} \end{bmatrix} \tag{30}$$

The alias matrix reveals much of the probability structure of the estimation procedure. From Equations 26, 28, 29 and 30 it can be seen that the standard deviation of the i^{th} adjusted gravity anomaly is the root sum square of the terms in the i^{th} row of the alias matrix. The elements in the first column of the alias matrix represent the R. S. S. contribution to the standard deviation of each estimated parameter due to the data noise. The elements in the J^{th} column, $J \geqslant 2$, represent the R. S. S. contribution to the standard deviation of each estimated parameter due to the $J - 1^{st}$ unadjusted parameter. These terms are called the aliasing contributions to the uncertainty in the adjusted parameters due to the uncertainty in the $J - 1^{st}$ unadjusted parameter. Notice that the aliasing contributions due to the J^{th} unadjusted parameter are proportional to the standard deviation of the J^{th} parameter. Definition: In a given estimation process the i^{th} estimated parameter is said to be orthogonal with respect to the J^{th} unestimated parameter if the aliasing contribution to the i^{th} estimated parameter due to the uncertainty of the J^{th} unestimated parameter is zero.

Two things can be noticed concerning this definition. First, the orthogonality relationship between two parameters must be defined within the context of a given estimation process. The data set must be defined and it must be stipulated which parameters are in the adjusted and in the unadjusted mode. Second, although we have been discussing mean free air gravity anomalies and altimeter data our mathematical results and definitions are applicable to any linear estimation problem where some parameters are adjusted and others left unadjusted.

To see the implications of the orthogonality relationship we need a more revealing representation of the aliasing terms. First notice that the first term on the right side of Equation 22 is the covariance matrix of the estimation process under the assumption that the unadjusted parameters are perfectly known. This covariance matrix gives the uncertainty of the estimates due only to data noise. Define the so-called "noise only" covariance matrix as

$$\bar{P} \equiv (A_1^T Q^{-1} A_1 + P_1^{-1})^{-1} \tag{31}$$

Next observe that the elements in the i^{th} row and J^{th} column of respectively A_1 and A_2 are the partial derivative of the i^{th} data point with respect to the J^{th} adjusted parameter and the partial derivative of the i^{th} data point with respect to the J^{th} unadjusted parameter. The aliasing contribution to the i^{th} adjusted parameter due to the J^{th} unadjusted parameter can be written as

$$L(I,J+1) = \sum_{K=1}^{n_1} \bar{P}(I,K) \sum_{L=1}^{m} \frac{\partial \delta\tilde{N}(L)}{\partial \delta\tilde{g}_1(K)} Q^{-1}(L,L) \frac{\partial \delta\tilde{N}(L)}{\partial \delta\tilde{g}_2(J)} \tag{32}$$

where m is the number of data points.

If the estimates of the adjusted parameters are relatively uncorrelated in the noise only covariance matrix, Equation 32 can be approximated by

$$L(I,J+1) = \bar{P}(I,I) \sum_{L=1}^{m} \frac{\partial \delta\tilde{N}(L)}{\partial \delta\tilde{g}_1(I)} Q^{-1}(L,L) \frac{\partial \delta\tilde{N}(L)}{\partial \delta\tilde{g}_2(J)} \tag{33}$$

A sufficient condition for the left side of Equation 21 to approximate zero is for the observability patterns of $\delta\tilde{g}_1$ (I) and $\delta\tilde{g}_2$ (J) in the data to be virtually non-overlapping. Up until about 40°, Stokes' function rapidly attenuates with increasing values of spherical radius.[4] Hence if the grids on which $\delta\tilde{g}_1$ (I) and $\delta\tilde{g}_2$ (J) are defined are sufficiently separated, the orthogonality relationship would be effectively satisfied and the estimate of $\delta\tilde{g}_1$ (I) would experience no aliasing from the uncertainty of $\delta\tilde{g}_2$ (J). Conversely if the grid on which $\delta\tilde{g}_1$ (I) was defined were in close proximity to grids whose gravity anomalies were unadjusted, one would expect serious aliasing of the resultant estimate.

It should be clear then, that if the gravity anomalies are estimated in a block the outer layers of the block contain gravity anomalies whose estimates will be badly aliased by the adjacent unadjusted parameters. It will be necessary to discard these estimates. But the gravity anomalies in a sufficiently small inner core of the block may be adequately separated from the unadjusted parameters to be effectively orthogonal with respect to them. The estimates of these terms presumably will be of sufficient accuracy that they can be accepted. In effect, for every block of gravity anomalies that we intend to estimate it will be necessary to construct a "buffer zone" several layers deep of gravity anomalies which surround the block. The new and larger block of gravity anomalies must be simultaneously estimated and then the estimates of gravity anomalies in the

buffer zone must be rejected due to aliasing. In order to achieve an intelligent compromise between estimation accuracy and computational load it is necessary to know the relationship between the depth of the buffer zone and the accuracy of the estimation procedure. The relationship will vary with grid size, computation radius and data density. The most convenient way to study the relationship is to utilize covariance analysis techniques to generate alias matricies for several situations and to attempt generalizations from the results. This is accomplished in the following section.

ESTIMATION STRATEGIES FOR GRAVITY ANOMALY DETERMINATION

The accuracy with which a given gravity anomaly is estimated from altimeter data is a function of many parameters. It is of course dependent on the accuracy and density of altimeter data. As explained in the previous section it is also dependent on the radial distance between the estimated gravity anomaly and the nearest gravity anomaly which is in the unadjusted mode. This parameter we call the estimation radius. Another parameter, the computation radius, is an important determinant of the accuracy of a gravity anomaly estimation. The computation radius sets the maximum distance from a given grid element over which data is to be processed in order to estimate the gravity anomaly defined on that grid element. Estimation accuracy does not necessarily increase with increasing computation radius. To see the reason notice that for a given estimation radius the covariance matrix of a set of estimated gravity anomalies is given by Equation 22 as the sum of a matrix which is dependent only on data uncertainty and a matrix which represents the aliasing effects from the unadjusted parameters. With increasing computation radius the elements of the first matrix must decrease but in general the elements of the matrix which conveys the aliasing effects will increase. This effect can be shown graphically by means of so-called aliasing maps. To obtain our aliasing maps of Figures 3 and 4, we simulate in a covariance mode a situation in which we describe the marine geoid by means of two degree by two degree gravity anomalies and we assume 12 alitmeter observations for each grid, each with an uncertainty of 1 meter. In Figure 3 we map the R.S.S. contribution in mgals to the uncertainty in the estimated gravity anomaly defined on the grid element in the lower left hand corner when the adjacent anomalies are assumed to be in an unadjusted mode and to have an a priori uncertainty of 50 mgals. The computation radius is 5°. Notice that the aliasing contributions decrease with the distance between the unadjusted parameter and the estimated parameter thus demonstrating the inherent orthogonality property of the gravity anomaly parameterization of the marine geoid. In Figure 4 the computation radius has been changed to 20° and the aliasing effect is seen to decrease much less radically.

To achieve an intelligent compromise between computational load and estimation accuracy it is necessary to determine the precise relationship between the accuracy of the estimate of a given gravity anomaly and the estimation radius and computation radius employed in the estimation procedure. To do this we assume that altimeter data existed at a density of three data points per one degree by one degree grid and that the uncertainty on the data was one meter. It was also assumed that unadjusted gravity anomalies had a standard error about zero of 50 mgal. This figure is conservative, a more realistic figure being 30 mgal[12]. No a priori estimate was assumed for estimated parameters. The effect of unadjusted parameters out to a spherical radius of 45° were included in the computations. Under these conditions Figure 5 provides the standard deviation in

1	1	1	1	1	1	1	1	1	1	0	0	0	0	0
2	1	1	1	1	1	1	1	1	1	1	1	0	0	0
2	1	1	1	1	1	1	1	1	1	1	1	1	0	0
2	2	2	2	2	2	2	1	1	1	1	1	0	0	0
3	2	2	2	2	2	2	2	2	1	1	1	1	0	0
3	3	3	3	2	2	2	2	2	2	1	1	1	1	0
4	3	3	3	3	3	3	2	2	1	1	1	1	1	1
5	4	4	4	3	3	3	2	2	2	1	1	1	1	1
5	5	4	4	4	4	3	2	2	2	2	1	1	1	1
6	6	6	5	5	4	3	3	2	2	2	1	1	1	1
8	8	7	6	5	5	3	3	3	2	2	2	1	1	1
10	10	9	8	6	5	4	3	3	2	2	2	1	1	1
18	19	14	9	7	6	4	4	3	3	2	2	1	1	1
31	26	19	10	8	6	5	4	3	3	2	2	2	1	1
	31	18	10	8	6	5	4	3	3	2	2	2	1	1

Figure 3. Alias Map for 2° by 2° Grids
and for 5° Computation Radius

4	4	4	4	4	4	4	3	3	3	3	2	2	2	1
4	4	5	5	5	5	4	4	4	3	3	3	2	2	2
5	6	6	6	6	5	5	5	5	4	4	3	3	2	2
6	7	7	7	7	7	6	6	5	5	4	4	3	3	2
8	8	9	9	8	8	8	7	7	6	5	4	4	3	3
10	10	11	11	11	10	10	9	8	7	6	5	4	4	3
12	14	14	14	14	13	12	11	10	8	7	6	5	4	3
15	16	17	17	16	15	14	13	11	9	7	6	5	4	4
17	19	19	20	19	17	16	14	12	10	8	7	6	5	4
19	22	22	22	21	19	17	16	13	10	9	7	6	5	4
22	24	25	24	22	21	19	16	14	11	9	7	6	5	4
25	28	28	26	24	22	19	17	14	11	9	7	6	5	4
28	32	30	28	25	22	20	17	14	11	9	7	6	5	4
36	34	32	28	24	22	19	16	14	11	9	7	6	5	4
	36	28	25	22	19	19	15	13	10	8	7	6	5	4

Figure 4. Alias Map in mgals for 2° by 2° Grids and for 20° Computation Radius

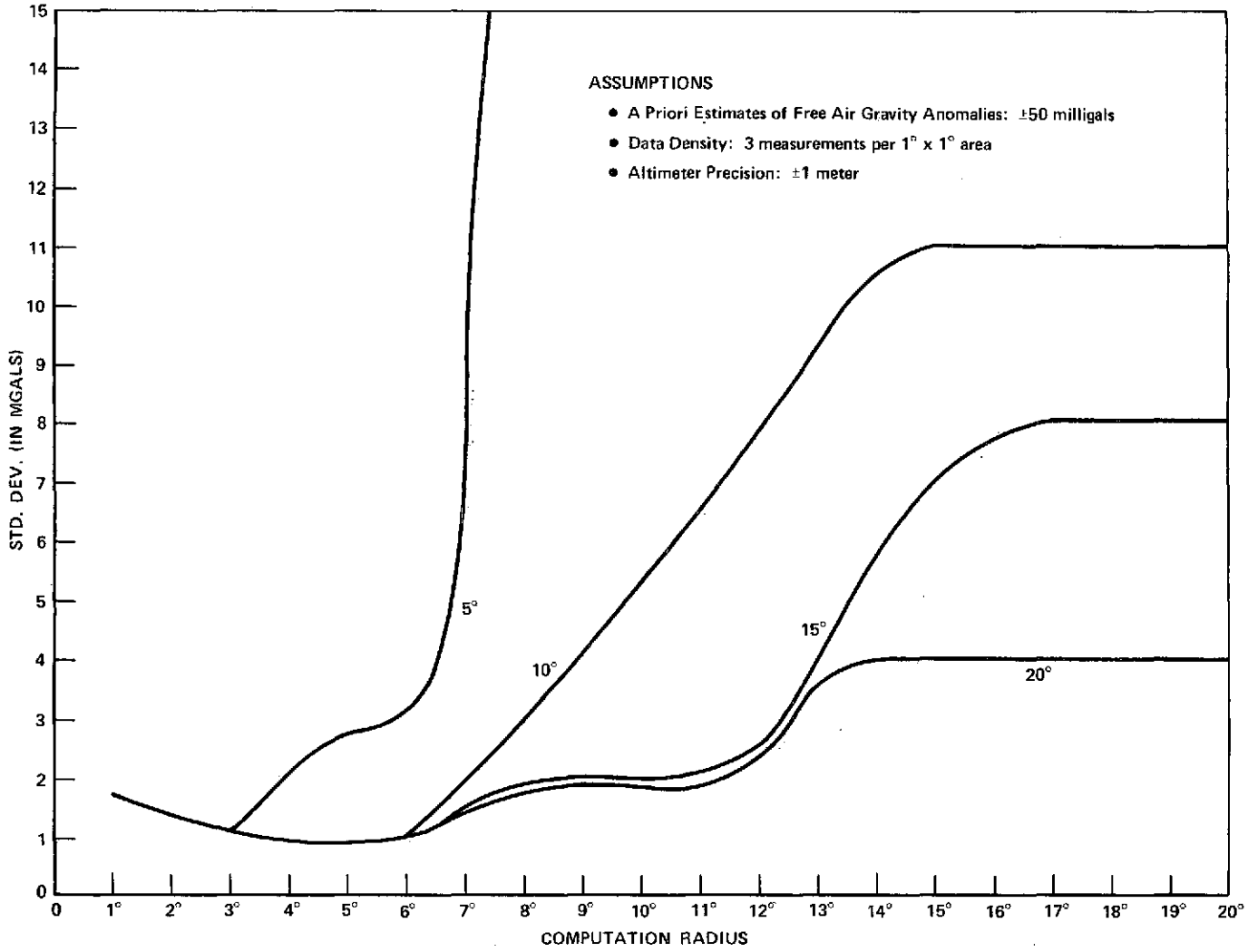

Figure 5. Accuracy of 5° by 5° Mean Free Air Gravity Anomaly Estimate vs. Computation Radius for Various Estimation Radii

the estimates of 5° by 5° mean free air gravity anomalies as a function of estimation radius and computation radius. From this figure it is clear that the most efficient estimation strategy for 5° by 5° anomalies is obtained with an estimation radius of about 10° and a computation radius of about 5°. This strategy will result in an accuracy of 1 mgal. This implies that if 5° by 5° mean free air gravity anomalies are estimated in blocks, estimates of gravity anomalies in the outer two layers of the block should be discarded due to aliasing. The rest of the estimated gravity anomalies should be accurate to within one mgal provided a 5° computation radius is used. It is important to remember, however, that our prime intent is to estimate a marine geoid rather than gravity anomalies. With estimates of 5° by 5° mean free air gravity anomalies can utilize Stokes' formula to analytically reconstruct a marine geoid which is sufficiently detailed that 5° features can be noticed. Since the discrete form of Stokes' formula is linear it is an easy matter to propagate a given error in gravity anomaly estimation into an error in marine geoid determination. Assuming that Stokes' formula is accurate if its summation is carried out within a 90° spherical radius of a given point, a one mgal standard deviation in the estimate of 5° by 5° mean free air gravity anomalies propagates into a 40 cm standard deviation of the resultant marine geoid. Thus by applying proper estimation procedures to the reduction of altimeter data should be possible to determine 5° features of the marine geoid with a resolution of 40 cm.

To obtain a more detailed marine geoid represents a more difficult estimation problem. Figure 6 provides the standard deviation in the estimates of 3° by 3° mean free air gravity anomalies as a function of estimation radius and computation radius. An estimation radius of 12° and a computation radius between 10° and 11° appears to provide the most intelligent estimation strategy. The strategy leads to estimates of 3° by 3° mean free air gravity anomalies which have standard deviations of 5 mgal. This implies that is 3° by 3° mean free air gravity anomalies are estimated in blocks, the outer 4 layers must be discarded as being badly aliased. A 5 mgal standard deviation in estimates of 3° by 3° mean free air gravity anomalies propagates into a standard deviation of 1.2 m in the resultant marine geoid. With the present assumptions no estimation strategy is adequate to determine features of the marine geoid as small as 2°. With much greater data densities such fine resolution is possible. For instance if we increase the data density by a factor of 100 thus postulating 300 data points for each 1° by 1° block, then with an estimation radius of 10° and a computation radius of 2°, 2° by 2° anomalies can be estimated with a standard deviation of 2.3 mgals. This propagates into a standard deviation of the marine geoid of about 42 cm. But to postulate such data densities is probably not realistic and in addition it suggests a very heavy computational load. The accurate resolution of 3° features of the marine geoid is likely to be the limit of what can be accomplished with altimeter data and the Stokes' formula mean free air gravity anomaly parameterization of the marine geoid.

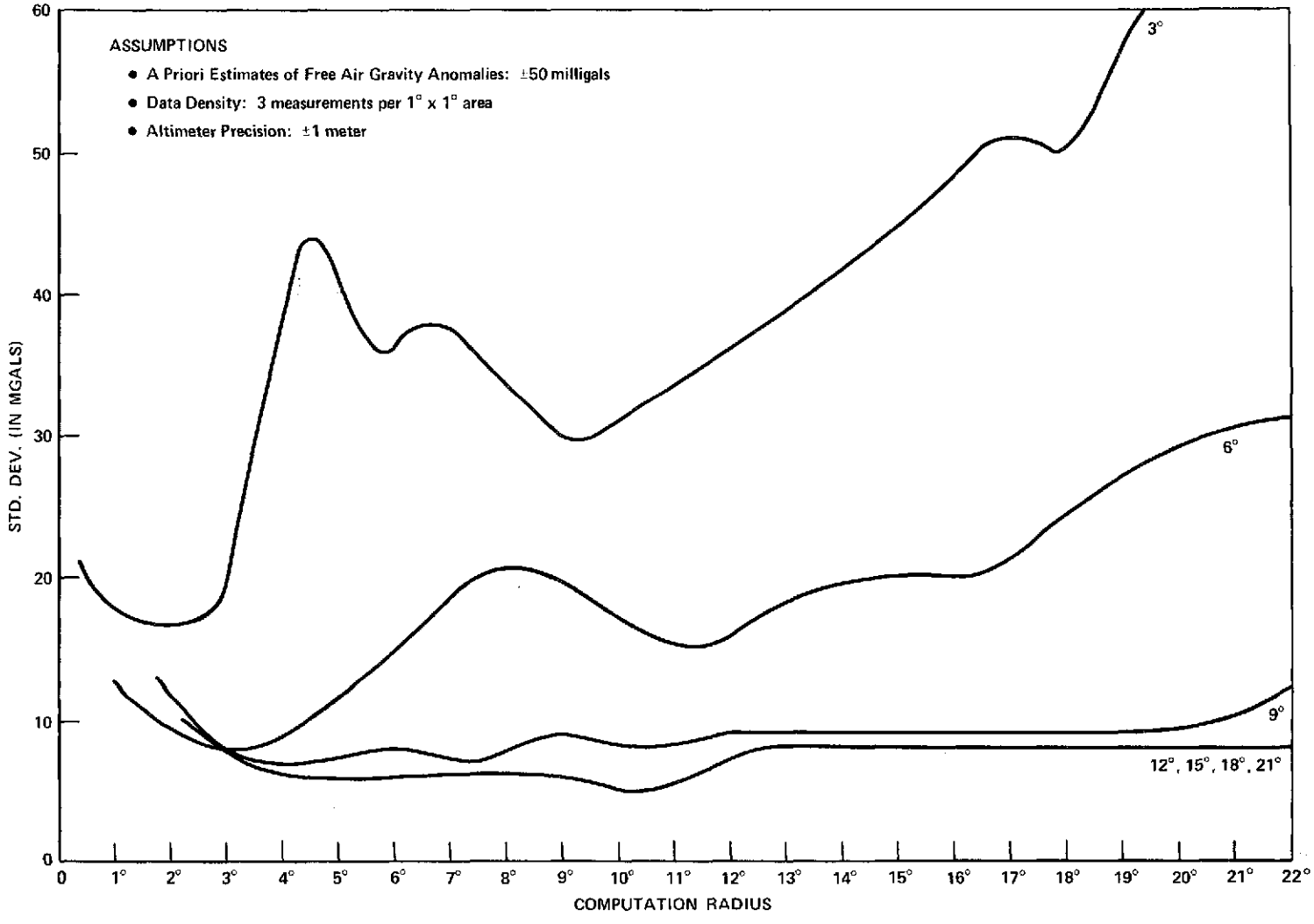

Figure 6. Accuracy of 3° by 3° Mean Free Air Gravity Anomaly Estimate vs. Computation Radius for Various Estimation Radii

Finally notice that these results were accomplished without assuming a priori estimates of gravity anomalies. In fact such estimates have been derived from satellite tracking data and direct gravity measurements. When these estimates are optimally combined with altimeter data by means of Equation 10 the resultant estimates of gravity anomalies will be predicted on all relevent data. The representation of the marine geoid derived from these estimates will then constitute the best possible estimate of that surface.

SUMMATION

Data from the SKYLAB altimeter has demonstrated the ability of altimetry to discerne the fine structure of the marine geoid. It will be during the GEOS-C mission, however, that global sensing of the sea surface topography from a spacecraft borne altimeter will be possible for the first time. In order to make optimal use of the vast amount of altimeter data expected from the GEOS-C one must apply numerous corrections to the data, both to eliminate systematic errors inherent in the data type itself and to correct for the effects of deviations of the mean sea surface from the marine geoid.

In order to employ standard parameter estimation techniques to estimate a marine geoid from altimeter data it is necessary to utilize a parameterization of the marine geoid which exhibits good orthogonality characteristics in the data type. In this respect at least, the Stokes' formula mean free air gravity anomaly parameterization appears to be the most promising. For a given grid size and data density, the accuracy of the geoid resulting from an estimate of gravity anomalies from altimeter data is a strong function of the choice of estimation radius and computation radius. An application of covariance analysis techniques reveals that assuming a data density of three measurements per one degree by one degree spherical surface area with each measurement accurate to within one meter, optimal choices of estimation radius and computation radius of respectively 10° and 5° yield an accuracy in the estimate of 5° by 5° mean free air gravity anomalies of approximately 1 mgal. This result implies that with a judicious choice of estimation strategy, one can determine geoid height with a standard deviation of 40 cm and a spatial resolution of 500 km (5 arc degree). With the same data density and data accuracy assumptions, covariance analysis demonstrates that optimal choices of 12° for estimation radius and 10° for computation radius permits one to estimate with an accuracy of approximately 1.2 m in geoid height with a spatial resolution of 300 km (3 arc degrees). Severe aliasing difficulties are encountered in attempting to estimate more detailed geoids. Our covariance analysis studies indicate, however, that a very small computation radius together with great data densities can mitigate the aliasing effects and yield in localized areas a marine geoid capable of showing spatial resolutions at the 100 km to 200 km level.

Finally it should be mentioned that by utilizing the Stokes' formula mean free air gravity anomaly parameterization of the marine geoid, it becomes an easy matter to combine satellite tracking data and direct measurements of gravity anomalies with altimeter data to obtain an optimal estimate of the marine geoid.

ACKNOWLEDGEMENT

The authors wish to thank Mr. J. T. McGoogan of NASA Wallops Station for providing the SKYLAB altimeter data used in this report.

REFERENCES

1. New York University School of Engineering and Science, Department of Meteorology and Oceanography, Report on Contract N62306-1589, U. S. Naval Oceanographic Office, Radar Altimetry from a Spacecraft and its Potential Applications to Geodesy and Oceangraphy, J. A. Greenwood, et al., May 1967.

2. NOAA, Technical Memorandum No. 59, The Earth's Gravity Field Represented by a Simple Layer Potential from Doppler Tracking of Satellites, K. R. Koch and B. V. Witte, April 1971.

3. Smithsonian Astrophysical Observatory, Report No. 294, Possible Geopotential Improvement from Satellite Altimetry, C. A. Lundquist, G. E. O. Giacaglia, K. Hebb, and S. G. Mair, 1970.

4. Heiskanen, W. A., and H. Moritz, Physical Geodesy, W. H. Freeman and Co., 1967.

5. Koch, K. R., Gravity Anomalies for Ocean Areas from Satellite Altimetry, Proceedings of the Second Marine Geodesy Symposium, Marine Technology Society, Washington, D. C., 1970.

6. Brown, R. D., and Fury, R. J., Determination of the Geoid from Satellite Altimeter Data, Goddard X document X-550-72-268, October 1972.

7. Argentiero, P., and Lynn, J., Estimation Strategies for Orbit Determination of Applications Satellites. NASA X document X-932-74-43, February 1974.

8. Hendershott, M. C., The Effects of Solid Earth Deformation on Global Ocean Tides, Geophys. J. R. Astr. Soc. (1972) 29, 389-402.

9. Saastamoinen, J., "The Use of Artificial Satellites for Geodesy" pp. 247-251; Geophysical Monograph 15. AGU 1972. "Atmospheric Correction for the Troposphere and Stratosphere in Radio Ranging Satellites."

10. Marsh, J., and Vincent, S., A Global Detailed Geoid, NASA X document X-592-73-266, August, 1973.

11. Deutch, Ralph, Estimation Theory, Prentice Hall, 1965.

12. Rapp, R. H., The Geoid Definition and Determination, Fourth G. E. O. P. Conference, University of Colorado, Boulder, August 1973.